

# Comparison of TOF and SL techniques for in-line measurement of food item volume using animal and vegetable tissues

Samuel Verdú <sup>a</sup>, Eugenio Ivorra <sup>b,\*</sup>, Antonio J. Sánchez <sup>b</sup>, Joel Girón <sup>a</sup>, Jose M. Barat <sup>a</sup>, Raúl Grau <sup>a</sup>

<sup>a</sup>*Departamento de Tecnología de Alimentos, Universidad Politècnica de València, Spain*

<sup>b</sup>*Departamento de Ingeniería de Sistemas y Automática, Universidad Politècnica de València,*

*Edificio 8G, Acceso D, Planta 1, Ciudad Politécnica de la Innovación, Camino de Vera, s/n, 46022 Valencia, Spain*

## Abstract

A comparison between the techniques Time of flight (TOF) and Structured Light (SL), for in-line process, was carried out to determine the volume of several food types with different compositions, structures and dimensions; 2 meat tissue (lean meat and pork fat) and 3 vegetable tissue (potato, apple and avocado). The volume obtained was compared with that determined by physical measurements, employing two statistical methods (a Bland-Altman study and partial least square analysis). Results showed that Structured Light (SL) was a better technique than Time of flight (TOF) for determining volume. The TOF technique was affected by factors which were more influential when the S/V ratio (surface of the sample exposed to the camera and sample volume) increased. SL was slightly affected by the composition of the sample. Fat content and the level of unsaturated fatty acids could be the reason for the reflection of the laser light on the surface of the samples thereby reducing the accuracy. Even so, the values of R<sup>2</sup> and RMSE of cross-validation, for the worst fit, demonstrated the quality of the SL technique.

## 1. Introduction

Developing new products and processes are primary objectives for the food industry to increase profits. To achieve these objectives it is necessary to incorporate new methods to enhance the quality, safety and efficiency of traditional processes (Datta & Halder, 2008). Non destructive analysis is an important approach which has wide areas of application. Groups of optical methods have recently been used to study some direct and indirect aspects of food products. 3D image systems are one of these groups. This group of systems applies different techniques, which will probably supplement 2-D machine vision based systems (Poussart & Laurendeau, 1988). In addition, 3D vision systems are solving challenging problems posed by conventional 2D imaging techniques (Mufti & Mahony, 2011), resulting in an increased interest and demand for this type of system. The 3D digitized geometry of food can be very interesting to model transformations and processes. For example, Fabbri, Cevoli, Romani, and Rosa (2011) used 3D models to describe numerical models of heat and mass transfer during coffee roasting. Trujillo and Pham (2006) used them to model heat and moisture transfer during beef chilling. Two different methods of obtaining 3D information are “Time of flight” (TOF) and “Structured light” (SL). The TOF technique (Xu, Schwarte, Heinol, Buxbaum, & Ringbeck, 1998) is based on a camera with a light which illuminates the scene with modulated, incoherent near infrared (NIR) wavelengths, and smart pixel sensors gather the reflected light (Keller & Kolb, 2009) whose return time is measured. A 3D model is generated through the contrast between empty scenes and scenes with object time variations. SL Technique is based on a laser projection of a specific pattern, for example a line on top of an object’s surface, the deformation of this pattern gives information about the surface of the object. This information is collected through a camera and processed to generate a 3D model. Both methods have so far been applied to very different areas. There are few TOF applications to measure 3D objects as this technology is mainly used for mobile robot applications, however this

technology could be applied successfully to measure the volume of objects (Ollikkala & Mäkynen, 2007) or even the morphology of plants (Klose, Penlington, & Ruckelshausen, 2009). Regarding SL, there are a lot of food applications such as food density prediction using acquired 3D information (Kelkar, Stella, Boushey, & Okos, 2011), 3D shape construction of tomatoes (Hatou, Morimoto, De Jager, & Hashimoto, 1996) or surface area and volume estimations of different food products (apple, pear, banana and strawberry) (Uyar & Erdogdu, 2009 ). But in these studies the volumes were obtained employing a 3D laser scanner with off-line data processing which means the technique is not suitable for working in an industrial application. The aim of this work was to study the viability of TOF and SL methods, working in-line, to calculate the volume of different foods using 3D models. Food samples with different matrices (animal and vegetable) and compositions were employed to evaluate possible influences on the volume obtained.

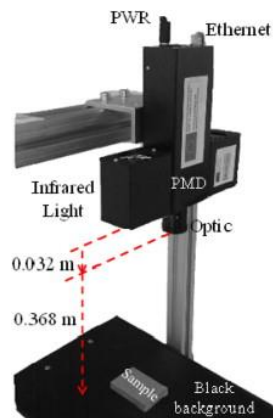


Fig. 1. 3D capture equipment based on time of flight.

## 2. Methods

### 2.1. Materials

Several types of food with different compositions, structures and dimensions were tested, 2 from meat tissue (lean meat and pork fat) and 3 from vegetable tissue (potato, apple and avocado). Wooden blocks were used as calibration objects since they are solid, have a regular shape and without brightness. For each type of food, five samples ( $n = 25$ ) were cut as cubic shapes with random sizes (from  $3.6 \text{ m}^3 \cdot 10^6$  to  $70.2 \text{ m}^3 \cdot 10^6$ ). Due to the difficulty of regular cuts on lean meat and fat samples, volume was calculated according to equation (1). In addition, for vegetable samples, volume was also calculated employing equation (2).

$$V = M.d \quad (1)$$

$$V = LWH \quad (2)$$

where L, W, and H represent the length, width, and height and M and d represent the weight and density. Density was calculated using a pycnometer.

### 2.2. Description of image acquisition device

#### 2.2.1. 3D using “Time of flight” method (TOF)

The Time of flight method is based on the calculation of the time that it takes an electromagnetic or other wave to travel a certain distance through a medium. Knowing the speed

of the wave in this medium, the distance can be calculated. In this case, the acquisition device used was the PMD[Vision] 19k camera (PMD Technologies GmbH, Siegen, Germany) (Fig. 1) which provides image and depth information about the scene. The camera sensor is based on CMOS technology formed by 19200 PMD (Photonic Mixer Devices) pixels with a resolution of 160 by 120. In each PMD pixel, the reflected infrared optical signal is correlated to the phase-shifted reference signal directly after charge generation in the photo diode, the distance is then calculated. For details about the features of the PMD imaging system and the phase shifting technique, see for example (Luan, 2001; Plaue, 2006). Image acquisition was conducted using three different points of view for each sample. It was performed rotating the samples so that all the edges (X, Y and Z) were in a vertical position. Rotation was done in order to take into account a possible influence between the exposed surface and the height of the sample. For each position 50 images were acquired using an integration time of  $5 \cdot 10^{-3}$  s and a frame rate of 1.5 frames per second (fps). Image acquisition was carried out without ambient light, using only the infrared light from the device to avoid noise from other light sources. The plane background used was a black plane at a distance of 0.4 m from the infrared light and 0.368 m from the optic. An image background was captured without samples in order to subtract this image from the images of the samples and obtain the samples height with positive values. For each sample position, a temporal filter from the median of 50 depth images and a spatial filter from the median of the pixels with a 9 9 window were carried out. Once the 3D image was filtered, the sample was segmented and its dimension and volume were calculated. A calibration process was carried out in order to transform the data acquired by the camera to international system units (SI).

### 2.2.2. 3D by “Structured light” method (SL)

The Structured-light method is based on the projection of a pattern of light on a sample and the calculation of 3D dimensions from the deformation of the pattern using a camera. In this case, the pattern used is a line projected by a red lineal laser (Lasiris SNF 410, Coherent Inc. Santa Clara, California (USA)) at a distance of 0.02 m. The camera (AD-080CL, JAI Company, Yokohama, Kanagawa (Japan)), working at 15 fps, was placed at 0.04 m above the conveyor belt. In addition, the camera was positioned so that the line laser projected on a unique row in the image. Both laser and camera were fixed and the 3D geometry was achieved by moving the sample on a conveyor belt with a constant speed of  $15 \cdot 10^{-4}$  m/s. The resolutions reached were  $3 \cdot 10^5$  m,  $1 \cdot 10^4$  m and  $10^3 \cdot 10^6$  m in the X, Y and Z axis respectively (Fig. 2). X resolution relies on the camera resolution and the distance to the sample; Y resolution depends on the speed of the conveyor belt and the camera's fps, so it could easily be improved if needed; and Z resolution depends on the angle between the camera and the laser. An angle  $\theta$  (Fig. 2) of  $38.675^\circ$ , as a compromise between Z resolution and a valid working range for the samples to analyse, was chosen. Samples were placed on the conveyor belt, one after another, in order to be scanned by the laser beam. To increase the information captured by the laser, samples were scanned twice, the second time rotated  $90^\circ$  around an axis formed by the normal vector surface. Calibration of the equipment was realized by taking 10 points regularly distributed in 3D in the laser projection plane (Trobina, 1995). Using these points with known 3D coordinates and their correspondent points in the image, a homography transformation was calculated (Zhang, 2000). The laser points projected on the image were extracted following these steps: first, the image was segmented using Otsu's global threshold (Nobuyuki Otsu, 1979), then the image was filtered removing non connected pixels with an area lower than 100px and finally, row coordinates were calculated by weight mean. This weight mean value was calculated for each column using the intensity value

in order to get subpixel precision. The 3D coordinates were then calculated using the homography and applying a rotation matrix in order to make the Z axis normal to the surface as can be seen in Fig. 2. Image processing methods, to extract volume information from TOF and SL, were calculated using own code developed employing Matlab R2012B (The Mathworks, Natick, Massachusetts, USA).

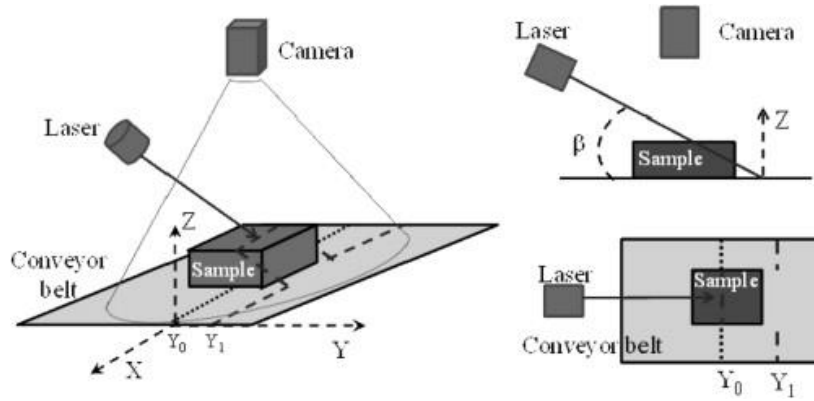


Fig. 2. 3D equipment capture based on structured light.

### 2.3. Statistical analysis

All parameters obtained were submitted to a Bland-Altman study (Martin Bland & Altman, 1986). This procedure is used to compare two different methods of measurement and to determine whether a new method of measurement could replace an existing accepted 'gold standard' method (Hill, Tofts, & Baldock, 2010). To provide additional information for comparison, a partial least square analysis (PLS) was carried out. The accuracy was given by the root mean square error (RMSE) and coefficient of determination ( $R^2$ ) for calibration (C) and cross validation (CV). Linear regression is the simplest and the most common tool used to assess systematic error (Gilbert, Barinov-Colligon, & Miksic, 1995). PLS is a method which finds a linear regression model by projecting measured variables and predicting values into a new space (Wold, Geladi, Esbensen, & Jerker, 1987). This algorithm has been proven to be a very powerful versatile data analytical tool applied in many areas of research and industrial applications (Rosipal & Krämer, 2006). The statistical analyses were all performed using Excel's Analysis Toolpack option (MS Corporation, Redmond, WA) and PLS Toolbox (Eigenvector Research Inc., Wenatchee, Washington, USA), a toolbox extension within the Matlab R2012B computational environment.

### 3. Results and discussion

The volumes of samples measured using physicochemical methods in relation to those measured employing the two 3D techniques used in this study are shown in Fig. 3. When the TOF method was used, three data sets were generated for each sample in response to the three different edge position captures, while two data sets were realized for each sample when the SL method was employed.

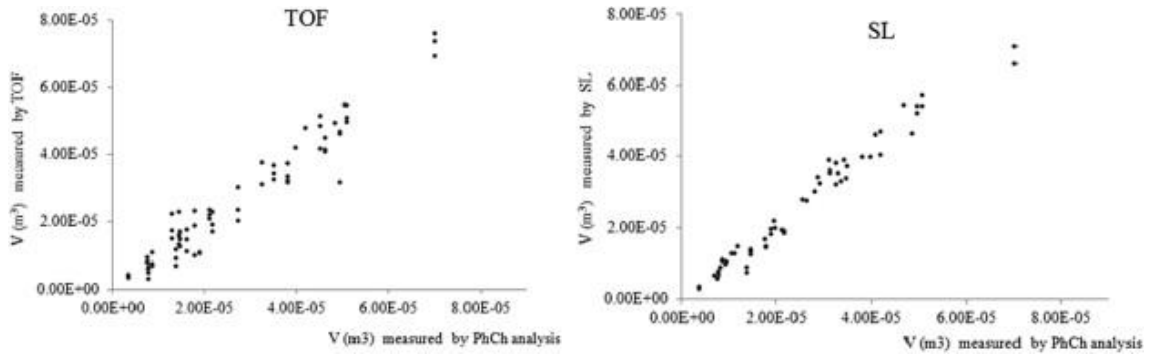


Fig. 3. Volume measured by physicochemical methods (PhCh) vs. volume measured using time of flight (TOF) or structured light (SL) for all samples.

Table 1. Bland–Altman study for data obtained from the two 3D techniques used vs. physicochemical analysis. The data presented are the thresholds (lower and upper limit) that include 95% of differences from the mean difference for each type of sample.

Product	TOF			SL		
	Lower	Upper	$\Delta$	Lower	Upper	$\Delta$
Wood	-2.64	3.42	6.06	-2.51	3.33	5.84
Lean meat	-10.77	5.17	15.94	-8.18	2.54	10.72
Pork fat	-3.63	6.44	10.07	-5.86	1.73	7.16
Avocado	-5.02	10.36	15.38	-0.54	7.07	12.61
Apple	-7.76	12.67	20.43	-4.7	6.25	10.95
Potato	-6.25	1.83	8.07	-6.24	7.03	13.27
All samples	-8.24	8.89	17.13	-6.82	5.2	12.02

As an example, Fig. 4 shows the 3D model built using SL and TOF techniques for lean samples. To assess the agreement between the two volumes from 3D techniques with those obtained by physicochemical methods, the data were statistically analysed using a Bland-Altman study and partial least square analysis. Table 1 shows the Bland-Altman study for both techniques used. The data presented are the thresholds that include 95% of the differences between the means of samples. As it is possible to observe, statistical results showed that the SL technique offered better results than TOF (lower difference between the thresholds for each type of sample) except for potato samples (DSL = 13.27; DTOF = 8.07).

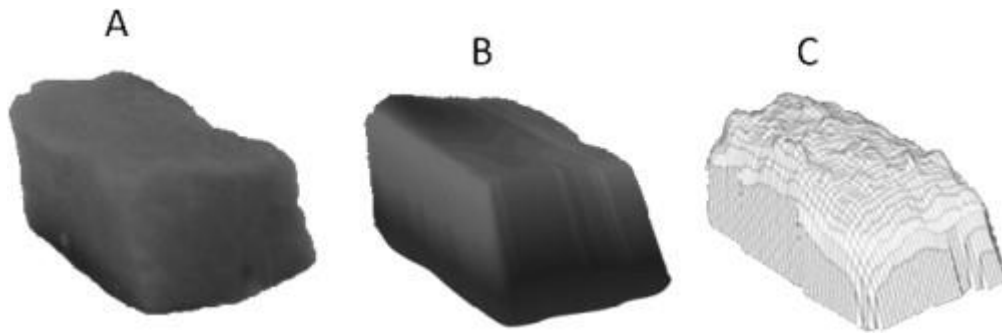


Fig. 4. (A) Sample of lean meat, (B) 3D image model using SL and (C) TOF techniques.

Calibration samples had similar results for both techniques (DSL = 5.84; DTOF = 6.06). When differences between thresholds, for each type of sample, were related to the main compound of the samples (fat, carbohydrates and water obtained from bibliography e USDA, 2012) or structure (vegetal or animal) no correlations were found independently of the technique used, so all data sets were statistically analysed. The thresholds interval (Table 1) showed that the SL technique was better (DSL = 12.02) than TOF (DTOF = 17.13) with lower data dispersion (Fig. 5).

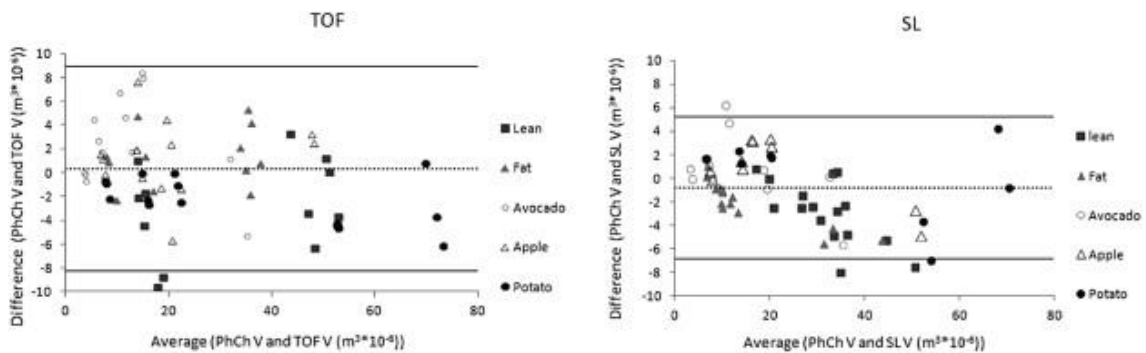


Fig. 5. Dataset Bland–Altman plot for both methods.

Table 2. Statistical results of the partial least square. Accuracy is given by the root mean square error (RMSE) and coefficient of determination ( $R^2$ ) for calibration (C) and cross validation (CV).

Product	TOF				SL			
	RMSEC	RMSECV	$R^2$ Cal	$R^2$ CV	RMSEC	RMSECV	$R^2$ Cal	$R^2$ CV
Wood	0.030	0.139	0.99	0.99	0.027	0.040	0.99	0.99
Lean meat	0.088	0.100	0.95	0.94	0.047	0.050	0.94	0.94
Pork fat	0.077	0.091	0.96	0.94	0.034	0.064	0.97	0.92
Avocado	0.097	0.123	0.87	0.81	0.066	0.088	0.94	0.91
Apple	0.111	0.122	0.88	0.86	0.035	0.044	0.98	0.98
Potato	0.024	0.028	0.98	0.98	0.043	0.056	0.98	0.98
All samples	0.139	0.141	0.85	0.85	0.066	0.070	0.94	0.94

RMSEC: Calibration Root Mean Square Error ( $m^3 \cdot 10^{-6}$ ).

RMSECV: Cross validation Root Mean Square Error ( $m^3 \cdot 10^{-6}$ ).

$R^2$  Cal: Calibration Correlation coefficient.

$R^2$  CV: Cross validation Correlation coefficient.

The statistical analysis using partial least squares of the data obtained employing both techniques indicate that the SL technique was better than TOF, reaching higher values for  $R^2$  CV and lower values for RMSE (Table 2). When the type of sample was related, a relationship was found when the SL technique was used. The worst fit was obtained for avocado and pork fat samples ( $R^2$  CV avocado = 0.91;  $R^2$  CV fat = 0.92) and the best for apple and potato ( $R^2$  CV = 0.98) while lean meat had intermediate values ( $R^2$  CV = 0.94). The fat content of the samples could be the reason for this behaviour. In fact, the fat on the surface of the samples produced a slight reflection of the laser light which reduced the accuracy measured from  $Y_0$  to  $Y$  (Fig. 6).

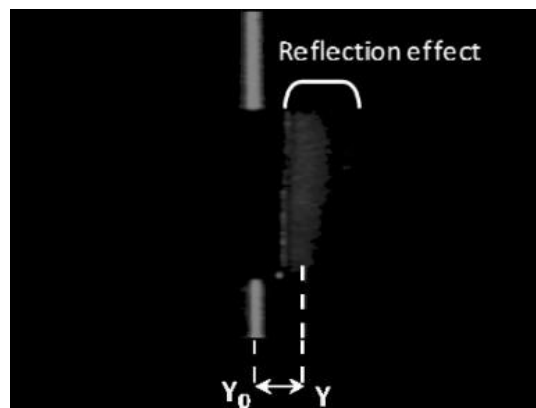


Fig. 6. Reflection effect generated by the fat on the surface of the sample.

It is possible that the reflection was higher for samples of avocado than for pork fat due to the higher level of mono and polyunsaturated fatty acids (USDA, 2012). There is greater data dispersion, using both statistical methods, when the TOF technique was employed (higher values

of RMSE). It could be due to some non-controlled factors which produced interactions with the reflected signal, modifying the flight time of the waves to the camera. In fact the error on the generated 3D model increased when the S/V ratio (surface of the sample exposed to the camera and sample volume) increased (Fig. 7). It could be explained by surface irregularities and the infrared reflexion coefficient of the samples, which would cause non returning light emissions and phase delays not related to distance (Mufti & Mahony, 2011). When shadow areas (not scanned), that may appear using SL technique, were studied, no statistical influence was observed. The 3D model generated and the volume obtained from it had similar values, independently of the scanning direction (Fig. 8). Further studies are necessary in order to evaluate the shadow areas in samples with irregular shapes. The timing cost required to determine the volume is divided into acquisition time and processing time. For TOF, acquisition time was limited by the slow FPS of this kind of device, in addition a large number of frames were necessary for the temporal median to reduce noise. On the other hand, SL had a higher FPS and only depended on the conveyor belt speed which is related to resolution.

#### 4. Conclusions

For in-line applications, Structured light (SL) was shown to be a better technique than Time of flight (TOF) for determining the volume of several foods with different composition, structure and dimensions, 2 from meat tissue (lean meat and pork fat) and 3 from vegetable tissue (potato, apple and avocado). The TOF technique was affected by some factors which had more influence when the S/V ratio (surface of the sample exposed to the camera and sample volume) increased. SL was slightly affected by the composition of the sample. Fat content and the level of unsaturated fatty acids could be the reason of the reflection of the laser light on the surface of the samples which reduced the accuracy. Even so the values of R2 and RMSE of cross-validation, for the worst fitting, demonstrate the aptness of SL technique for determining the volume. Further studies are needed to evaluate samples with irregular shapes and different tissues as well as time-resolution studies to adapt the application to in-line process.

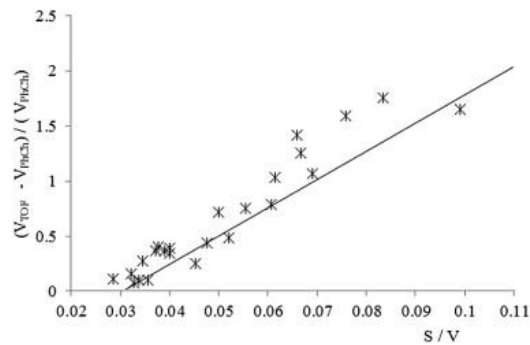


Fig. 7. Relationship between the S/V ratio (surface of the sample exposed to the camera and sample volume) and the error between the volume obtained from the TOF (V<sub>TOF</sub>) and from the physicochemical measures (V<sub>PhCh</sub>).



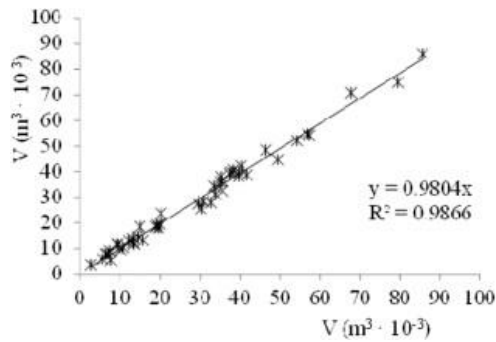


Fig. 8. Relationship between volumes obtained with SL technique depending on the scanning direction.

## 5. Acknowledgements

We wish to thank the Polytechnic University of Valencia and Generalitat Valenciana for the financial support they provided through the PAID-06-08-3251 and GVPRE/2008/170 Projects, respectively.

## 6. References

- Datta, A. K., & Halder, A. (2008). Status of food process modeling and where do we go from here (synthesis of the outcome from brainstorming). *Comprehensive Reviews in Food Science and Food Safety*, 7(1), 117e120.
- Fabbri, A., Cevoli, C., Romani, S., & Rosa, M. D. (2011). Numerical model of heat and mass transfer during roasting coffee using 3D digitised geometry. In 11th International congress on engineering and food (ICEF11): Vol. 1(0) (pp. 742e 746).
- Gilbert, M. T., Barinov-Colligon, I., & Miksic, J. R. (1995). Cross-validation of bioanalytical methods between laboratories. In *Papers from the fifth international symposium on pharmaceutical and biomedical analysis*: Vol. 13(4e5) (pp. 385e394).
- Hatou, K., Morimoto, T., De Jager, J., & Hashimoto, Y. (1996). Measurement and recognition of 3-D body in intelligent plant factory. In *International conference on agricultural engineering (AgEng)*. Madrid, Vol. 2, (pp. 861e862).
- Hill, R. F., Tofts, P. S., & Baldock, C. (2010). The BlandAltman analysis: does it have a role in assessing radiation dosimeter performance relative to an established standard? *Radiation Measurements*, 45(7), 810e815.
- Kelkar, S., Stella, S., Boushey, C., & Okos, M. (2011). Developing novel 3D measurement techniques and prediction method for food density determination. In 11th International congress on engineering and food (ICEF11), Vol. 1(0), (pp. 483e491).
- Keller, M., & Kolb, A. (2009). Real-time simulation of time-of-flight sensors. *Simulation Modelling Practice and Theory*, 17(5), 967e978.
- Klose, R., Penlington, J., & Ruckelshausen, A. (2009). Usability study of 3D Time-of-flight cameras for automatic plant phenotyping. *Bornimer Agrartechnische Berichte*, 69, 93e105. Luan, X. (2001).

Experimental investigation of photonic mixer device and development of TOF 3D ranging systems based on PMD technology. Universitätsbibliothek. Martin Bland, J., & Altman, D. (1986). Statistical methods for assessing agreement between two methods of clinical measurement. Originally published as Volume 1, Issue 8476, 327(8476), 307e310.

Mufti, F., & Mahony, R. (2011). Statistical analysis of signal measurement in time-of-flight cameras. ISPRS Journal of Photogrammetry and Remote Sensing, 66(5).

Nobuyuki Otsu. (1979, enero 1). A threshold selection method from gray-level histograms. IEEE Transactions on Systems, Man, And Cybernetics, SMC-9(1).

Ollikkala, A. V. H., & Mäkynen, A. J. (2007). Use of time-of-flight 3D camera in volume measurement. In Proceedings of SPIE, Vol. 7022, (pp. 702219).

Plaue, M. (2006). Technical report: Analysis of the PMD imaging system. Interdisciplinary Center for Scientific Computing, University of Heidelberg.

Poussart, D., & Laurendeau, D. (1988). Advances in machine vision. In J. L. C. Sanz (Ed.) (pp. 122e159). New York, NY, USA: Springer-Verlag New York, Inc. Rosipal, R., & Krämer, N. (2006).

Overview and recent advances in partial least squares. In C. Saunders, M. Grobelnik, S. Gunn, & J. Shawe-Taylor (Eds.), Vol. 3940 (pp. 34e51).

Berlin/Heidelberg: Springer Trobina, M. (1995). Error model of a coded-light range sensor. Technique Report. Communication Technology Laboratory.